Host galaxies and environments of compact extragalactic radio sources

Labiano Ortega, Alvaro

2

Compact and extended radio sources in the southern sky

Preliminary version of a paper to be co-authored by:
A. Labiano, P.D. Barthel, R.W. Hunstead, R.T. Schilizzi, J. Bland-Hawthorn

We present Very Large Array (VLA) observations of a subset of southern extragalactic sources selected from the Molonglo Southern 4 Jy (MS4) Sample, demonstrating that MS4 is comparable to the northern Third Cambridge Revised catalogue. Several interesting individual objects are discussed, including new galactic sized CSS objects. New CSS sources are found: B0614–349, B0615–365, B0646–398, B0707–359, B1015–314, B2259–375 and B2339–353 as well as a CSS candidate in the core of B0618–371.

2.1 Introduction

In the last fifty years, several surveys in radio wavelengths have been performed. The most used and better studied is the Third Cambridge Catalogue (3C; Edge et al. 1959) and its revisions (3CR and 3CRR; Bennett 1962; Laing et al. 1983). The 3C catalogues were made selecting radio sources (both galactic and extragalactic) with $S_{178MHz} \geq 10\,\mathrm{Jy}, \delta \geq 10°, |b| \geq 10°$. The latest revision, 3CRR (Laing et al. 1983) comprises almost two hundred extragalactic radio sources. The majority (85%) are large FR I (edge darkened, Fanaroff & Riley 1974) and FR II (edge brightened) radio sources. 15% of the 3CRR sample are Compact Steep Spectrum (CSS) sources (Nan et al. 1991; Sanghera et al. 1995) and no Gigahertz Peaked Spectrum (GPS) sources are found (see Table 2.2 for more detailed statistics). The absence of GPS sources in the 3CR catalogues is most likely due to the spectral shape of these sources: the position of the peak makes them too faint around 178MHz to be included in the 3C catalogues. They are however generally present in radio source samples selected at cm or dm wavelengths (e.g de Vries et al. 1997b)

The 3C catalogue was the first detailed catalogue of extragalactic radio sources. It has been used extensively in the last 50 years, and still is. However, there was no equivalent of the 3C catalogues in the southern sky until 1998, when R.W. Hunstead and A.M. Burgess (Burgess 1998) presented a comparison sample in the southern hemisphere: the Molonglo Southern 4 Jy Sample (see also Burgess & Hunstead 2006a).

2.2 The Molonglo Southern 4 Jy Sample

The Molonglo Southern 4 Jy Sample (MS4) consists of 229 radio sources selected from the 408 MHz Molonglo Reference Catalogue (MRC; Large et al. 1981), with a flux density $\gtrsim$ 4 Jy. It covers declinations between –85° and –30° and a galactic latitude $|b| > 10°$. The Magellanic Clouds were excluded because sources found there would be very complicated to identify as extragalactic. The 229 sources in MS4 were imaged with the Molonglo Observatory Synthesis Telescope (MOST) at 843MHz at a resolution of 43" × 43"cosec δ, yielding radio positions accurate to a few arcsec, crude angular sizes and flux densities. Sources with angular sizes < 35" were imaged at 5 GHz with the Australia Telescope Compact Array (ATCA) in snapshot mode at a resolution of 2–8". The optical identifications were done using UK Schmidt plates for the brighter objects and AAT[1] *R*-band CCD images for the fainter ones, along with the MOST and ATCA positions. Only half of the MS4 sources, mostly quasars and nearby galaxies, have published spectroscopic redshifts (after optical identification, e.g., Burgess 1998). Optical magnitudes were used to estimate the redshift of the sources without spectroscopic data (see column 13 of Table 2.1). Comparing the MS4 and 3CRR catalogues should be, in principle, straightforward, as both catalogues cover equivalent regions of the sky and the flux density limits (10 Jy at 178 MHz and 4Jy at 408 MHz) are comparable for a spectral slope $F \propto \nu^{-1}$.

[1] Anglo-Australian Telescope

2.3 VLA observations of MS4 compact sources

In order to increase the number of known GPS and CSS sources, study basic radio parameters (e.g. angular size) and test number statistics, we observed a complete sub-sample of the MS4 catalogue using the Very Large Array (VLA) in the X-band (3.5 cm), with the BnA configuration. We obtained 1" resolution images of 26 MS4 sources with angular size between $\sim$2 and $\sim$30 arcsec, in the –30° to –40° declination strip. The strip contains 74 sources in total. In addition to our 26 sources, there are 39 radio sources with size $>$ 30" and 9 with size $\lesssim$ 2".

2.4 Data reduction and mapping

The 26 southern MS4 radio sources were observed with the VLA, in its BnA configuration, on June 24 and 26, 1998, employing the standard X-band (8.4GHz, 2x50MHz) receiver system. Two snapshots of typically ten minutes each, at different source hour angles were made. Each program source was observed with an associated phase calibrator, whereas calibrator 3C 286 was used to establish the absolute flux scale. The BnA configuration (east and west arms in "B", the second longest configuration, and the northern arm in "A", the longest configuration), of the VLA was chosen to optimize the beam shape for observations of sources in the southern sky. The typical beamsize in the final images is 1 x 0.5 arcsec (see Table 2.1). The radio data were of high quality, and there was no need for extensive flagging of discrepant data points. Reduction of the data was performed using standard NRAO AIPS image processing routines, including several steps of self-calibration (phase only, followed by amplitude self-calibration). Several successive self-calibration and cleaning cycles generally led to a rapid convergence towards the images presented below. The resulting radio maps are shown in figures 2.3 to 2.7. Figures 2.8 and 2.9 present overlays of the radio maps and available optical *R*-band images. Table 2.1 summarizes the source and map properties.

2.5 Notes on individual sources

Before discussing the sample properties, we proceed by describing the individual sources imaged with the VLA. The spectral indices have been estimated using our VLA observations (8.4 GHz) and the MOST measurements (843MHz) for the integrated emission of the source. ATCA data (4.8 GHz) were used to estimate the spectral indices of the cores (Table 2.1). We assume that the spectra of the sources behave as a power law between the available frequencies. Many of the sources in our strip only had observations with MOST.

B0012–383: Lobe dominated triple source associated with an intermediate redshift galaxy (z=0.65). ATCA observations show just the lobes while our observations bring up a possible core, consistent with the optical observations (Figure 2.8). Both lobes show tails of extended emission and misalignment of the three components.

B0036–392: ATCA observation showed a double source associated with an optical quasar. Our observations confirm it but reveal a structured center of the source with a big twist, almost in a "z" shape.

B0042–357: ATCA observations showed a compact asymmetric double source associated with a z_R =1.259 (Burgess 1998) galaxy: a very bright spot in the south with extended bright emission to the north. Our higher resolution map shows that this extended emission is a compact bright component separated ∼50 kpc from the southern component, aligned north-south with the other component.

B0157–311: A highly structured source with very extended emission and several hot spots, associated with a quasar. Burgess (1998) identifies the central, brightest component as the core of the source. We compute $\alpha_{4.8}^{8.4} \simeq -0.4, (\mathrm{F} \propto \nu^{-\alpha})$, which could be produced by the variability of the core, resolution effects or contamination from the extended emission in our estimation of the flux density. The complex structure of the radio jets suggests a dense ISM.

B0340–0372: A CSS source ($\alpha_{0.843}^{8.4} \simeq 1$) with several compact components aligned in the NE-SW direction and extended emission to the NW. The optical identification corresponds to a quasar coincident with the central component of the VLA map (White et al. 1988).

B0411–346: The ATCA map shows a single bright component CSS source ($\alpha_{0.843}^{8.4} \simeq 1$) in the radio map of this z∼1 galaxy. Our higher resolution separates the source in two components.

B0427–366: An extended, linear triple source with some faint extended emission towards the south of the central component. The ATCA map showed a lobe dominated triple source connected by extended emission. The optical image (Burgess & Hunstead 2006b) shows a stellar source slightly south of the central component but there is no available spectrum for the source so it could be classified as a quasar candidate.

B0601–344: A faint compact source, associated with a galaxy, with some faint extended emission towards the north east. There are no ATCA maps of this source. The MOST map showed a similar morphology.

B0602–319: A bright source with a peak in the center and extended emission to the south. The shape of the central component suggests an unresolved secondary component. Higher resolution maps would be needed to check it. Burgess (1998) suggests that the brightest radio component is the core of the quasar but we estimate $\alpha \sim 2$ which seems too far from the flat, expected, value.

B0614–349: An unresolved CSS source associated with a galaxy. We compute a spectral index $\alpha_{0.843}^{8.4} \simeq 0.66$.

B0615–365: An unresolved CSS source, $\alpha_{0.843}^{8.4} \simeq 0.91$, associated with an optical galaxy.

B0618–371: The VLA map shows a very extended source with two components separated ∼30 arcsec, associated with a galaxy. The brightest component is also very compact and the eastern component shows extended emission, probably the end of the jet. There are

no good estimations of the flux density of the Western (compact) component which could be the core and/or a CSS source. Parma et al. (1991) shows a wider field map of this source revealing a 2' long triple, almost symmetric, FR II source with very wide extended emission around the lobes. Parma et al. (1991) place the optical counterpart (a b_J = 14.8 dumb-bell galaxy) in our VLA compact component.

B0646–398: An unresolved faint CSS source, computed $\alpha_{0.843}^{8.4} \simeq 2$, associated with a possible quasar (no optical spectrum of the optical -compact- counterpart). The high value of the spectral index can be due to variations in the emission of the source.

B0707–359: An unresolved CSS source for which we compute $\alpha_{0.843}^{8.4} \simeq 1.8$ with a bright optical galaxy counterpart. As with the previous source, the high value of the spectral index can be due to variations in the emission of the source.

B1015–314: An unresolved CSS source, $\alpha_{0.843}^{8.4} \simeq 0.86$, with a quasar counterpart.

B1206–337: A highly aligned four component source associated with a faint distant galaxy. ATCA observations only reveal two components. Our map shows two faint hotspots between the brightest components. The optical overlay indicates the absence of a radio core.

B1247–401: A highly structured lobe dominated source with a galaxy counterpart. ATCA observations only reveal two components, which we manage to separate. Our map suggests a twist in the center of the source but it can be due to the shape of the beam.

B1346–391: ATCA observations show a $\sim 8''$ double source that our higher resolution reveals as a triple source. The southern component seems to be made of two radio components which we do not resolve completely. The optical image shows emission close to the compact component in the center of the radio map. We only compute an upper limit to the spectral index of the possible core: $\alpha_{4.8}^{8.4} < 1.3$.

B1359–358: ATCA observations suggest a $\sim 8''$ double source associated with an optical galaxy. We resolve both components and some extended emission between them.

B1955–357: The ATCA map shows a double source which we separate into a three component source with the central component coincident with the optical quasar counterpart suggesting we are resolving a core (with $\alpha_{4.8}^{8.4} < 2.2$) and two lobes.

B2049–368: A $\sim 5''$ compact double both in the ATCA and our map, associated with a galaxy. The beam shape makes it very difficult to interpret the map. Burgess (1998) places the core in the southwestern component ($\alpha_{4.8}^{8.4} < 1.1$).

B2128–315 A triple source with a compact lobe component in the south west and an extended component with two compact bright components towards the north east. The optical position of the quasar coincides with the central radio component suggesting a core (although we compute $\alpha_{4.8}^{8.4} \simeq 1$) and two lobes, the northern one connected to the core by jet emission.

(1)	(2)	(3)	(4)	(5)	(6)	(7)	(8)	(9)	(10)	(11)	(12)	(13)	(14)	(15)	(16)	(17)
Source	RMS	Beam Size	Beam Angle	Peak Flux	$S_{8.4}$	$S_{0.843}$	α	$S_{c,4.8}$	$S_{c,8.4}$	α_{core}	Type	z	LAS	LSS (kpc)	PA	CSS?
B0012-383	4.84E-05	1.25 x 0.52	29.00	8.95E-02	0.14	2.18	1.2	<55	1.1	<7	G	0.650*	28.8	199	56	
B0036-392	1.14E-04	1.81 x 0.87	22.98	5.97E-02	0.18	2.75	1.2	177:	50	2	Q	0.592	10.8	71	44	
B0042-357	1.99E-04	1.54 x 0.54	22.35	4.06E-01	0.54	3.73	0.8	<251	<39	–	G	1.259*	7.5	63	175	
B0157-311	1.57E-04	0.82 x 0.53	38.14	1.63E-01	0.74	5.62	0.9	130:	168	–0.4	Q	0.677	53.6	377	174	
B0340-372	9.82E-05	0.93 x 0.64	-9.77	4.23E-02	0.34	3.09	1.0	–	–	–	Q	0.2844	8.3	35	63	
B0411-346	2.85E-04	0.88 x 0.62	-25.18	1.09E-01	0.20	2.3	1.0	–	–	–	G	1.027*	3.7	30	105	CSS
B0427-366	5.46E-04	1.83 x1.21	-62.5	3.41E-02	0.14	3.69	1.4	–	4.1	–	Q?	0.456	24.6	142	166	
B0601-344	1.48E-03	4.57 x 3.87	-8.89	5.68E-02	0.11	2.52	1.4	–	–	–	G	0.662*	15.7	110	27	
B0602-319	3.60E-04	1.07 x 0.96	-54.5	2.24E-01	0.64	3.93	0.8	815	243	2.2	G	0.452	11.6	63	23	
B0614-349	1.11E-03	0.84 x 0.59	-40.81	6.74E-01	0.82	3.73	0.7	–	–	–	G	0.329	U	U	U	CSS
B0615-365	4.88E-04	1.12 x 0.74	-22.20	3.26E-01	0.36	2.92	0.9	–	–	–	G	1.580*	U	U	U	CSS
B0618-371	9.48E-05	0.81 x 0.64	-26.81	1.51E-02	0.04	3.8	2.0	–	17	–	G	0.0326	38.9	25	84	core?
B0646-398	5.38E-04	2.19 x 0.85	-51.82	1.52E-02	0.03	3.85	2.1	–	–	–	Q?	0.78**	U	U	U	CSS
B0707-359	1.53E-04	0.92 x 0.6	-35.26	4.96E-02	0.06	3.42	1.8	–	–	–	G	0.327*	U	U	U	CSS
B1015-314	2.60E-03	2.02 x 0.43	-45.66	7.10E-01	0.75	5.49	0.9	–	–	–	Q	1.346	U	U	U	CSS
B1206-337	9.62E-05	1.84 x 0.9	22.61	2.85E-02	0.087	2.18	1.4	<33	<3	–	G	1.672*	19.4	167	149	
B1247-401	8.24E-05	1.52 x 0.66	10.42	5.12E-02	0.12	2.56	1.3	<49	3.0	<5	G	1.610*	9.8	84	32	
B1346-391	8.33E-05	1.07 x 0.62	19.40	5.69E-02	0.25	2.97	1.1	<111	53	<1.3	G	0.690*	10.4	74	16	
B1359-358	7.43E-05	0.88 x 0.61	28.65	1.24E-01	0.20	2.56	1.1	<122	<40	–	G	0.594*	8.6	57	45	
B1955-357	1.02E-04	1.93 x 0.42	38.51	1.54E-01	0.37	2.8	0.9	<210	61	<2.2	Q	0.36	10.7	53	170	
B2049-368	6.90E-05	1.68 x 0.44	36.67	8.84E-02	0.12	5.75	1.7	<73	40	<1.1	G	1.124*	6.8	56	39	
B2128-315	5.93E-05	1.15 x 0.45	39.83	5.74E-02	0.27	4.18	1.2	106	61	1	Q	0.99	8.8	70	141	
B2226-386	6.91E-05	1.37 x 0.5	29.59	1.45E-01	0.15	8.21	1.7	<110	147	<-0.5	G	1.776*	7.3	62	169	
B2259-375	1.83E-04	1.16 x 0.53	29.05	4.76E-01	0.55	7.47	1.1	–	–	–	G	1.504*	U	U	U	CSS
B2323-407	1.78E-04	1.48 x 0.51	27.69	7.72E-01	1.07	9.28	0.9	<1	0.7	<0.6	G	0.996*	18.7	149	35	
B2339-353	6.64E-05	1.13 x 0.51	32.20	1.37E-01	0.24	5.67	1.4	–	–		G	0.635*	U	U	U	CSS

Table 2.1–. Summary of the VLA observations at 8.4 GHz and BnA array. (1) Source name. (2) Image RMS noise in mJy/beam. (3) Size of the beam in arcsec. (4) Angle of the beam in degrees (North to East). (5) Peak flux in the continuum image (Jy/beam). (6) Flux density at 8.4GHz, measured with VLA, in Jy, measured from the images by adding up the clean components making up the source emission. (7) Integrated flux density at 0.843 GHz, measured with MOST, in Jy (from Burgess 1998). (8) Spectral index, α, if F $\propto \nu^{-\alpha}$, calculated from columns 6 and 7. (9) Flux density (in mJy) at 4.8 GHz, from ATCA maps (Burgess 1998) of the possible core of the source; ";" means some extended emission surrounding the core is included in the measurement, upper limits are three times the RMS in this region. (10) Flux density from the VLA maps (8.4GHz) in mJy of the possible core of the source. All the sources, except B0012-383 and B2323-407, have the core surrounded by considerable extended emission so the exact values are uncertain. (11) Spectral index of the possible core, calculated with columns 9 and 10. No attempt was made to estimate the flux density in CSS sources. Negative values are probably due to overestimation of the 8.4 GHz flux, due to extended emission, underestimation of the 4.8 GHz upper limits or variability of the core. (12) Optical identification: galaxy (G) or quasar (Q). (13) Redshift of the source, from Burgess (1998). * means estimated from R magnitude, ** means estimated from b_J magnitude. (14) Largest angular size in arcsec. (15) Largest linear size of the source in kpc. A size or angle marked "U" means the source is unresolved. (16) Position angle in degrees. (17) Identification of CSS sources according to size and spectral index. Although B0618-371 is almost 40 kpc long, the west component (the possible core) could be a CSS source.

B2226–386: A double source, associated with an optical galaxy, with a bright component in the south and a fainter hotspot in the northern connected by some faint extended emission. Burgess (1998) places the core of this source in the southern, brightest component, for which we compute $\alpha_{4.8}^{8.4} < -0.5$. This negative value can be due to variability of the core or overestimation (due to "contamination" from the surrounding extended emission) of our 8.4GHz flux density.

B2259–375: An unresolved CSS source, $\alpha_{0.843}^{8.4} \simeq 1.1$, with a galaxy counterpart.

B2323–407: A lobe dominated triple source with a very faint central component, coincident with the optical galaxy, suggesting a core ($\alpha < 0.6$).

B2339–353: An unresolved CSS source, $\alpha_{0.843}^{8.4} \simeq 1.4$, associated with an optical galaxy.

2.6 Results

Table 2.2 shows a summary of the occurrence of galaxies, quasars and CSS/GPS sources in the 3CRR catalogue (173 sources) and the strip between $-30° < \delta < -40°$ from the MS4 (74 sources out of the 229 of the complete catalogue). We have used the redshifts and identifications of optical counterparts in Burgess (1998). We define a CSS source to have projected linear size $\lesssim$ 15 kpc (H_0 = 71 km $s^{-1}Mpc^{-1}$ and $\Omega_\Lambda = 0.73$, Ω_M = 0.73) with $\alpha > 0.5$, and GPS sources those with size below 1 kpc. We have classified the unresolved objects as CSS sources. Higher resolution imaging would be needed to classify them as GPS. The complete MS4 catalogue only has two sources classified as GPS so far (B0008–421 and B1934–638), 0.9% of the total sample. Our VLA observations reveal several CSS sources: B0411–346, B0614–349, B0615–365, B0646–398, B0707–359, B1015–314, B2259–375 and B2339–353. The core of B0618-371 may harbor a CSS source too, although more spectral data is needed to confirm it. The data for the 3CRR have been taken from Laing et al. (1983) and http://www.3crr.dyndns.org/, as well as Nan et al. (1991) and Sanghera et al. (1995) for the CSS occurrences.

About 8% of the MS4 strip has not been identified as quasar or galaxy, therefore the percentages of each type in the sample can change when the remaining objects are classified. Ignoring these unidentified sources, the MS4 strip and the 3CRR catalogue have the same fraction of galaxies ($\sim$76% and $\sim$75% respectively) and the MS4 strip lacks of quasars (16%) compared to the 3CRR (25%). If most of the unidentified objects in the MS4 strip were classified as quasars, the occurrence be similar to the 3CRR quasars. However, the complete MS4 catalogue lacks of quasars (20%) compared to the 3CRR (25%).

Regardless of optical identification, both catalogues show a similar occurrence of CSS sources (15% in the MS4 strip and 15% in 3CRR) and lack GPS sources. The lack of GPS sources can be due to their spectrum (steep and peaked at $\sim$ 1 GHz), as GPS are expected to be weak at low frequencies. There is a clear discrepancy in the occurrence of CSS galaxies and quasars in both catalogues: almost all the CSS sources in the MS4 strip are galaxies

Object	ID	MS4 strip	Stat. Err.	3CRR	Stat. Err.	Ratio
Complete Sample	Total	74 (100%)	0	173 (100%)	0	2.3
	Galaxies	56 (76%)	4	129 (75%)	6	2.3
	Quasars	12 (16%)	3	43 (25%)	6	3.6
	Unidentified	6 (8%)	2	1 (<1%)	1	0.17
CSS	Total	11 (15%)	3	26 (15%)	5	2.4
	Galaxies	9 (12%)	3	12(7%)	3	1.3
	Quasars	2 (4%)	1	14(8%)	4	7.0
GPS	Total	0	0	0	0	–

Table 2.2–. Statistics of the different objects in MS4 and 3CRR. Comparison between the different object IDs in the 3CRR and our MS4 $-40< \delta <-30$ sample. The first part of the table gives the numbers for the total samples and the second part the CSS and GPS statistics. Columns *Stat. Err.* give the statistical errors associated to the number of sources in each category. The last column gives the ratio 3CRR / MS4 of identification in each sample for each type of object. We also give the percentage to the total sample for each object. MS4 statistics from our VLA data and Burgess (1998). 3CRR statistics from Laing et al. (1983) and http://www.3crr.dyndns.org/.

while CSS sources are evenly spread in galaxies and quasars for the 3CRR. This discrepancy can be due to the definition of the optical counterparts in MS4 which would confuse, for instance, broad line galaxies, galaxies with compact appearance, quasars with narrow line spectra or with extended emission (Burgess 1998).

Figure 2.1 shows the distribution of sizes in the MS4 strip and the complete 3CRR catalogue. The behavior is similar: high occurrences of small sources and decreasing with size. Both catalogues show a trend to increase around the 350 kpc region, although the MS4 strip seems to lack sources between 350 and 400 kpc. Otherwise, the distribution is, in general, similar, specially taking into account that we are using low number statistics. Burgess (1998) finds comparable linear size distribution for the sources in the complete MS4 and 3CRR so we must attribute this "gap" between 350 and 400 kpc to the selection of just a strip in the sky instead of the complete MS4 catalogue or the low number statistics. The Kolmogorov-Smirnov test seems to support the similarity of catalogues. However, it is not conclusive (Figure 2.2).

2.7 Summary

We carried out at comparison study between a MS4 strip and the 3CRR catalogue and improved the classification of CSS sources in the MS4 catalogue. We find that although there are slight differences, these are mainly due to small number statistics; both catalogues show the same general distributions. The $-30^\circ < \delta < -40^\circ$ strip of the MS4 catalogue is more abundant in CSS galaxies but contains fewer CSS quasars. The MS4 strip also lacks sources with diameters between 350 and 400 kpc compared to the 3CRR.

We find new CSS sources in the MS4 strip: B0614–349, B0615–365, B0646–398, B0707–359, B1015–314, B2259–375 and B2339–353 and a CSS candidate in the core of B0618–371.

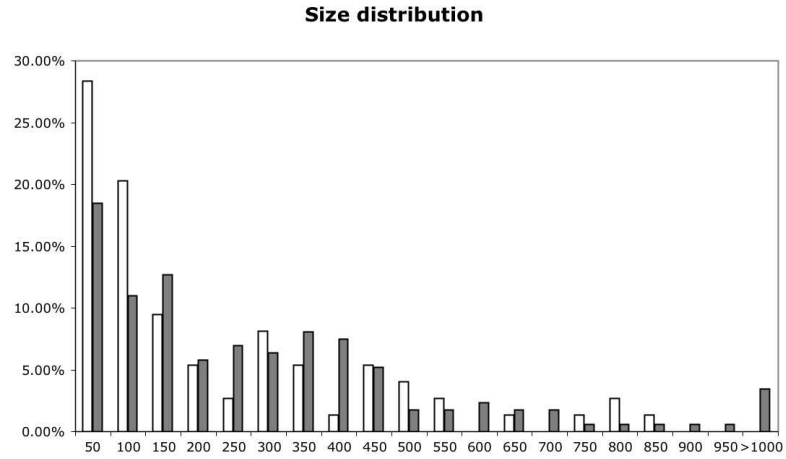

Figure 2.1–. Comparison of the distribution of sizes (in kpc) in the 3CRR (shaded bars) and MS4 strip (white bars) samples:173 and 74 radio sources respectively. The sources have been grouped in 50 kpc bins. The first column contains all the sources with sizes below 50 kpc; the second one sizes between 50 and 100 kpc, and so on. The last column represents sources with sizes bigger than 1 Mpc.

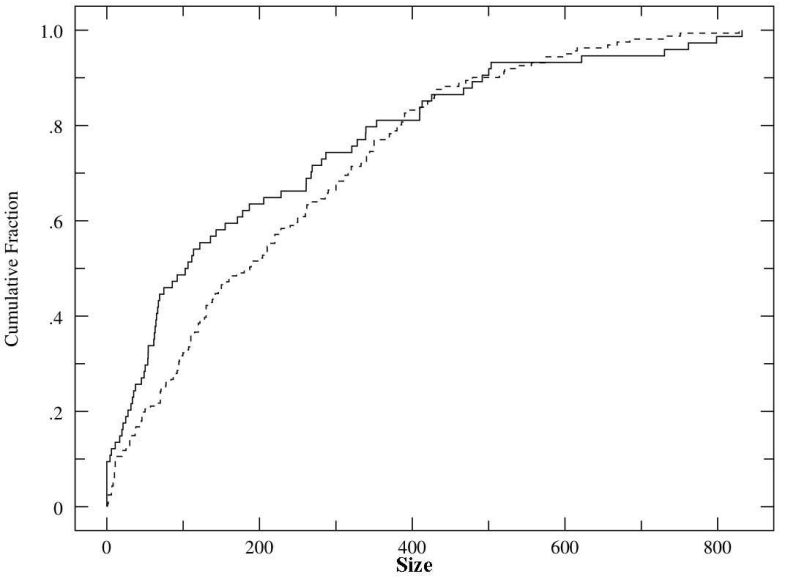

Figure 2.2–. Cumulative histogram for sizes of MS4 strip (solid line) and 3CRR (dashed line) sources.

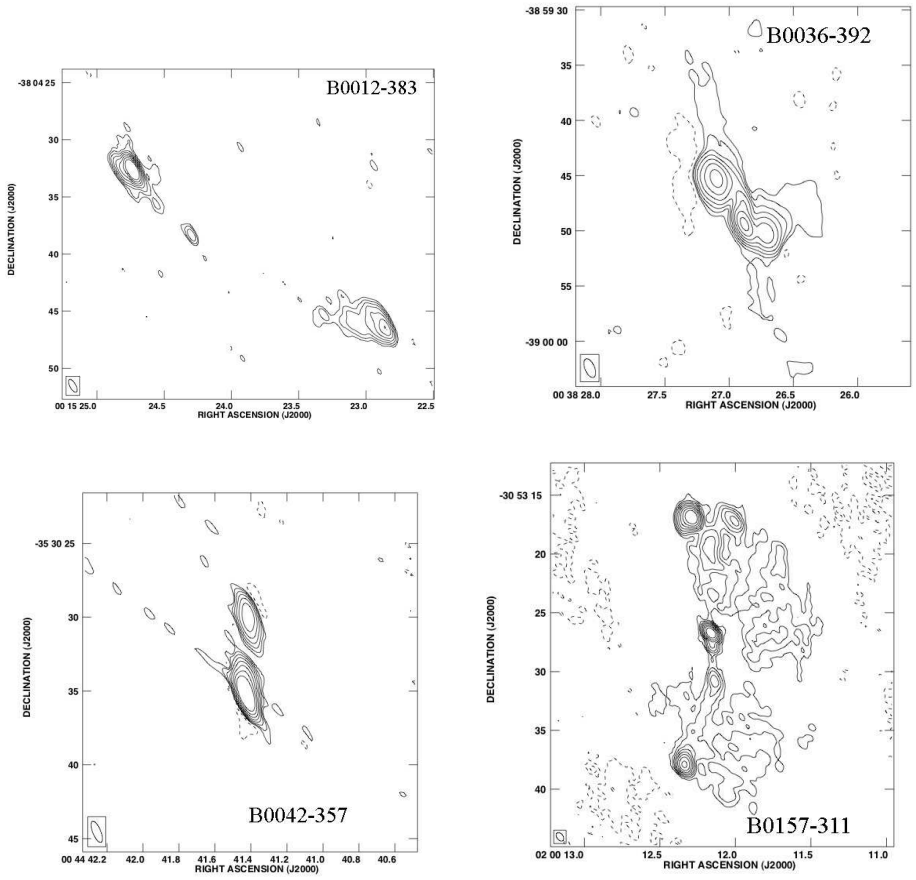

Figure 2.3–. VLA 8.4GHz maps of MS4 sources. Contours are -3, 3, 6, 12, 24, 48, 96, 192, 384 multimples of the rms noise in the images (see table 2.1). Typical noise levels of ∼0.1% peak flux were reached. Only resolved sources are shown.

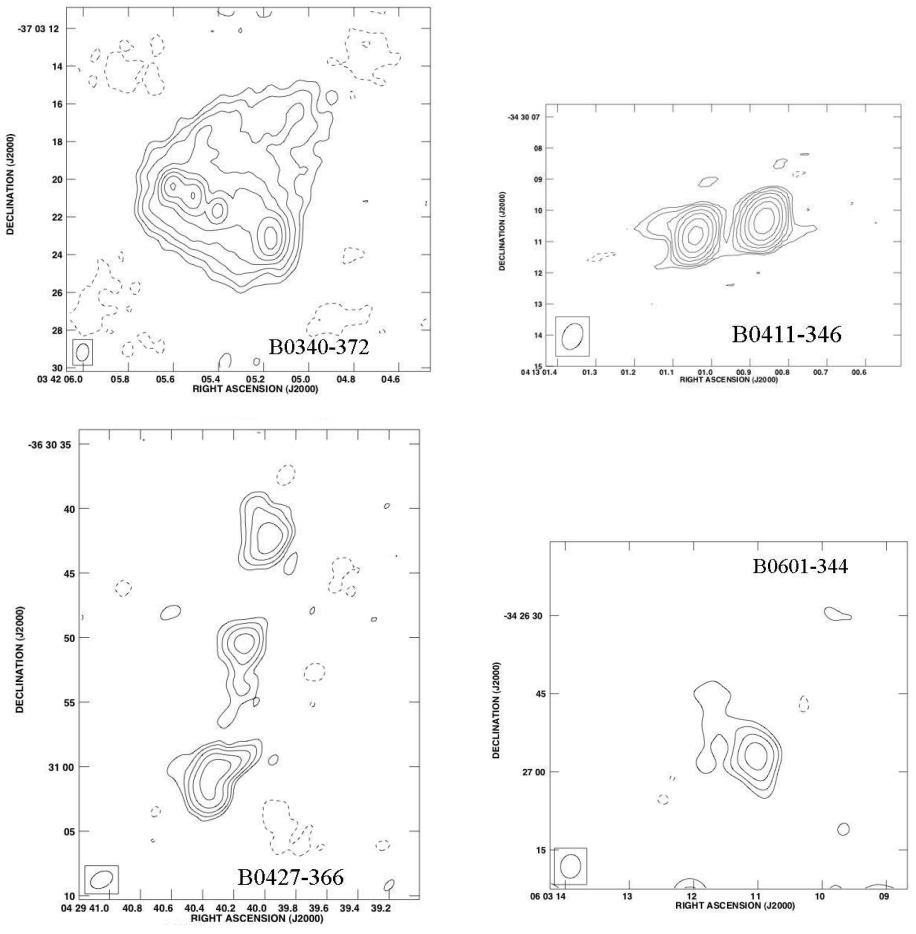

Figure 2.4–. Same as Figure 2.3.

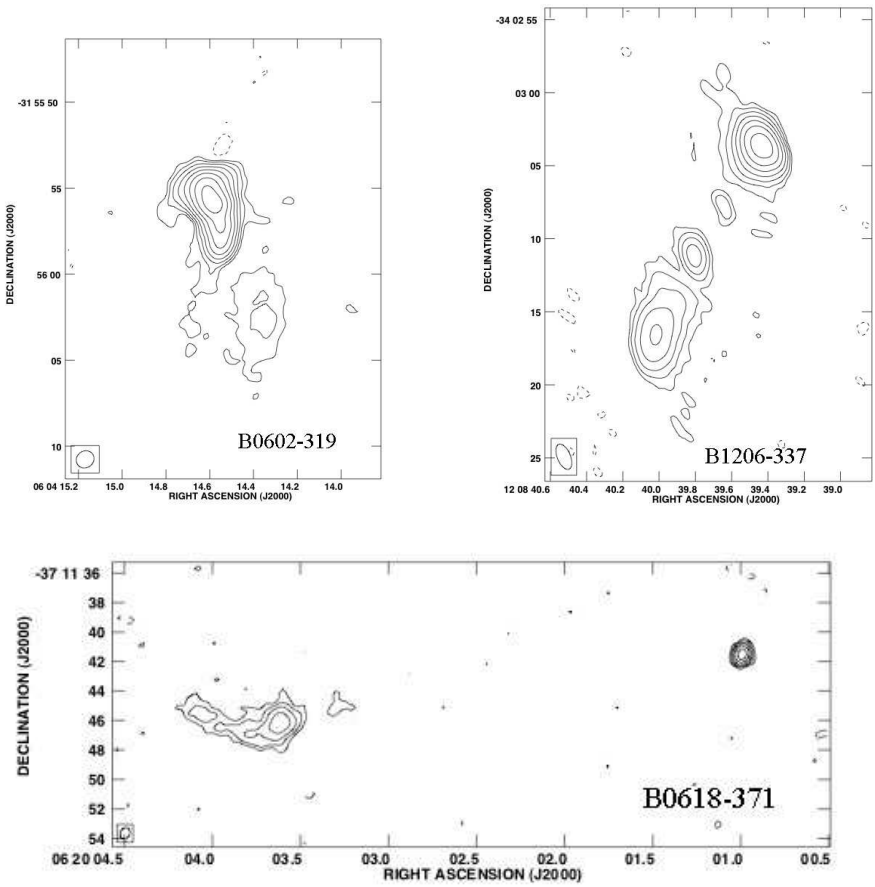

Figure 2.5–. Same as Figure 2.3.

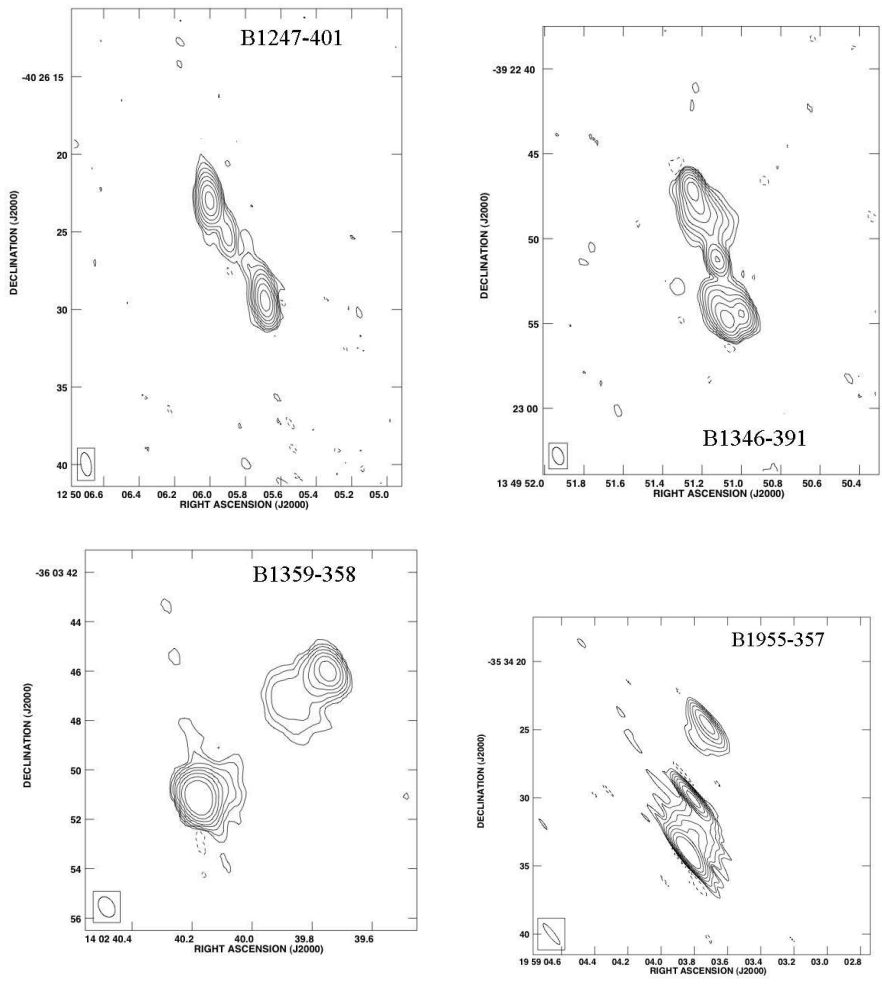

Figure 2.6–. Same as Figure 2.3.

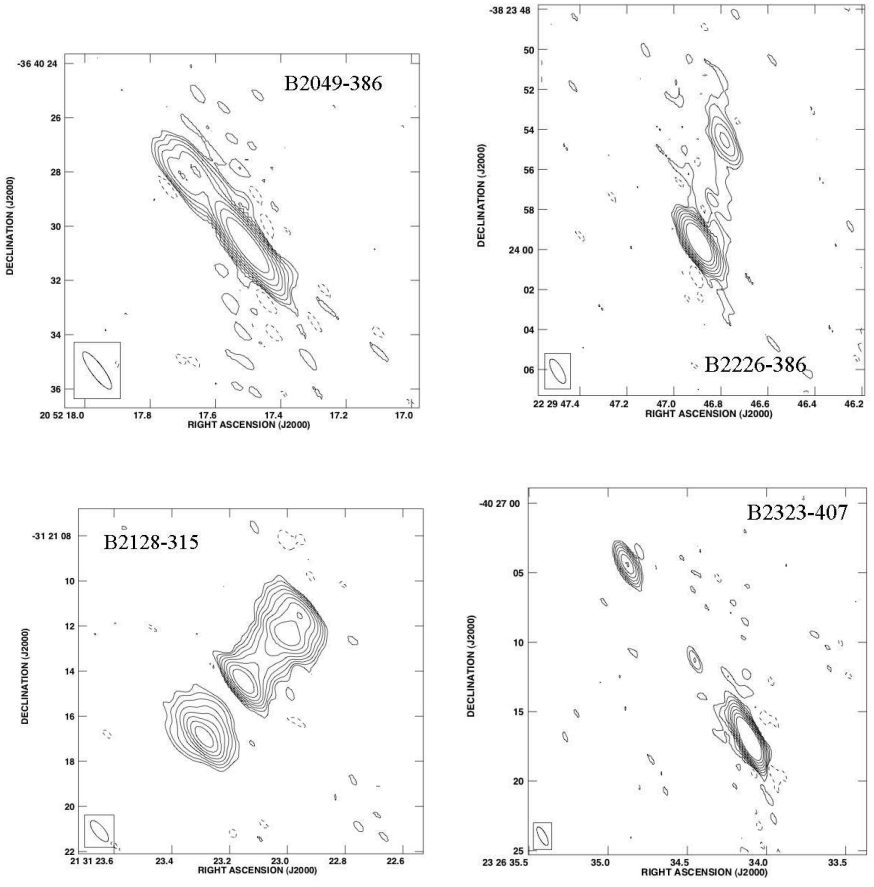

Figure 2.7–. Same as Figure 2.3.

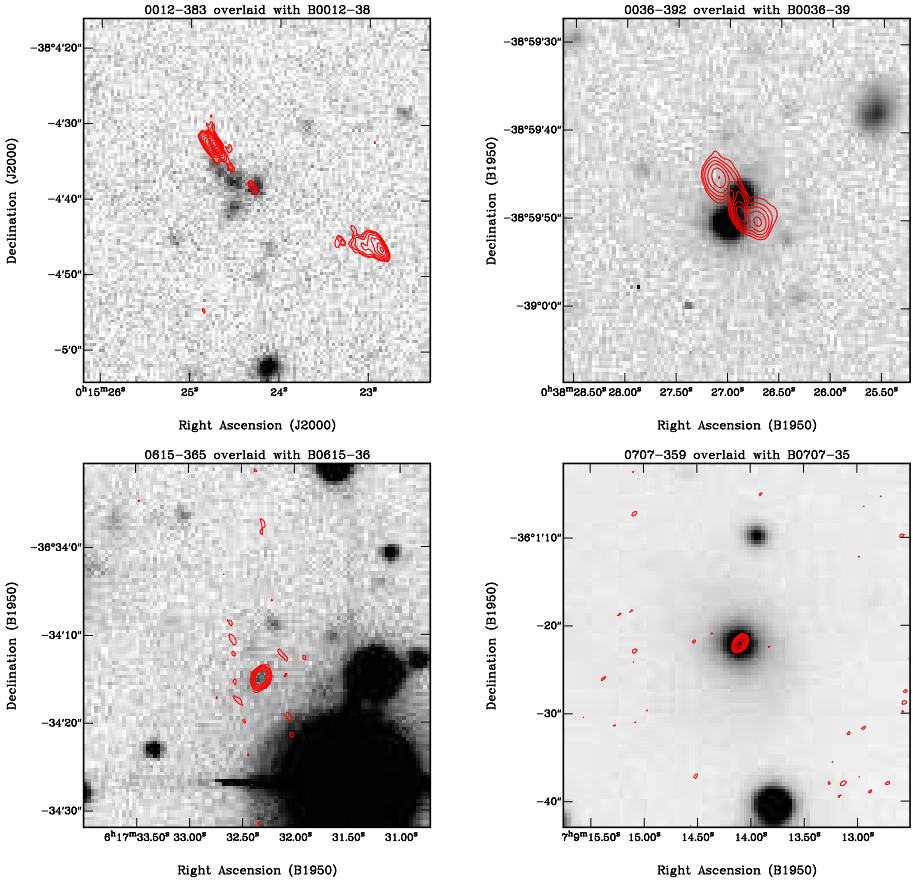

Figure 2.8–. Overlays of our VLA images and *R*-band overlays of MS4 sources observed with the Anglo-Australian Telescope.

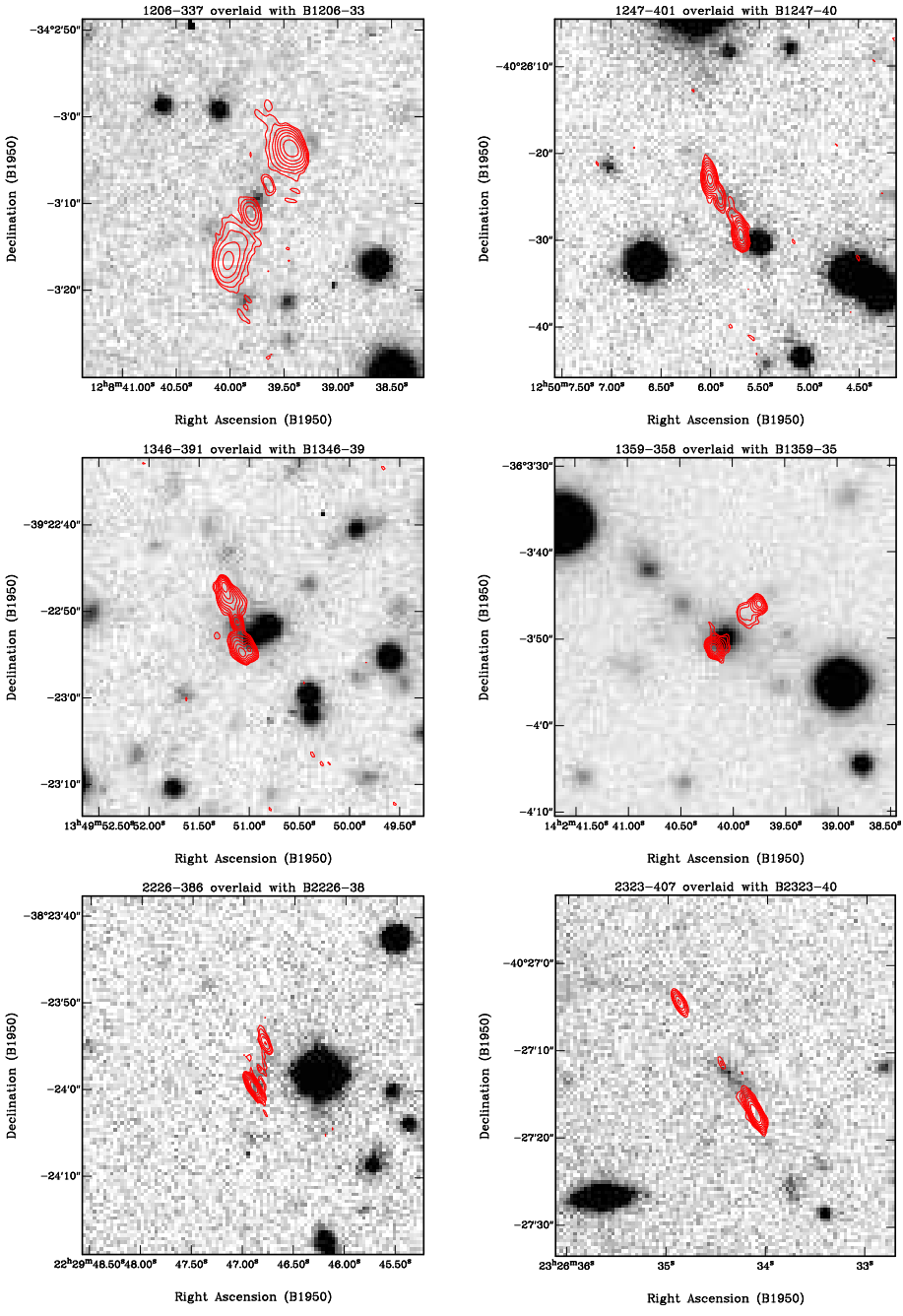

Figure 2.9–. Same as Figure 2.8.